Owen, A., Ebinghaus, A., Hartley, A. J., Santos, M. G.M. and Weissmann, G. S. (2017) Multi-scale classification of fluvial architecture: an example from the Palaeocene-Eocene Bighorn Basin, Wyoming. Sedimentology, 64(6), pp. 1572-1596.

http://eprints.gla.ac.uk/144080/

Deposited on: 12 July 2017

Multi-scale classification of fluvial architecture: an example from the Palaeocene-Eocene Bighorn Basin, Wyoming

Amanda Owen[1], Alena Ebinghaus[1], Adrian J. Hartley[1], Maurício G.M. Santos[2], Gary S. Weissmann[3]

[1] Geology and Petroleum Geology, School of Geosciences, University of Aberdeen, Aberdeen, UK.

[2] CECS, UFABC, Santo André, Brazil.

[3] Department of Earth and Planetary Sciences, University of New Mexico, Albuquerque, NM, USA.

Corresponding author email: a.owen@abdn.ac.uk **Address**: Department of Geology and Petroleum Geology, School of Geosciences, University of Aberdeen, Aberdeen, AB24 3UE, U.K.

Abstract

Fluvial channel geometry classification schemes are commonly restricted in relation to the scale at which the study took place, often due to outcrop limitations or need to conduct small-scale detailed studies. A number of classification schemes are present in the literature; however there is often limited consistency between them, making application difficult. The aim of this study is to address this key problem by describing channel body geometries across a depositional basin to ensure a wide range of architectures are documented. This was achieved by studying 28 locations over 4000 m of vertical succession in Palaeocene and Early-Eocene aged deposits within the Bighorn Basin, Wyoming, USA. Five different channel body geometries have been defined based on the external geometric form, and internal arrangement and nature of storey contacts. These include the Massive channel body body geometry, Semi-amalgamated channel body geometry, Internally amalgamated channel body sheet geometry, Offset stacked channel body geometry, which are considered to be subdivisions of the sheet geometry' of many other classifications. An Isolated channel body geometry has also been recognised alongside a channel and sheet sandstone geometries in the floodplain facies associations. Field evidence, including the stacking style of storey surfaces, suggests that the different geometries form a continuum. The nature and degree of amalgamation at the storey scale is important in producing the different geometries, and is related to degree of channel migration. It is speculated that this is the result of differences in sediment supply and available accommodation. In contrast to previous schemes, the classification scheme presented here recognises the importance of transitional geometries. This geometrical range has been recognised because of the basin-scale nature of the study.

(1) Introduction

Alluvial architecture assesses the lateral and vertical variations in grain size, geometry, and proportion of channel and floodplain deposits (Allen, 1978). Understanding variations in alluvial architecture has important economic implications as fluvial deposits are known to be economically important (i.e. petroleum, groundwater and mineral resources, CO_2 sequestration). Understanding alluvial architecture also has important implications for palaeogeographic reconstructions. Key controls on alluvial architecture include intrinsic (i.e. avulsions, bar form migration, local sediment supply at the reach scale) and extrinsic processes (i.e. base level variations, tectonics and climate) (Bridge, 2008; Cecil, 2013). As these different processes can act at a range of scales and magnitudes, and are often interrelated, predicting the characteristics of alluvial architecture can be challenging. Indeed even effectively describing alluvial architecture can be challenging as it requires large scale, well exposed outcrops,

40 and/or sufficient seismic data quality and coverage, and an abundance of closely-spaced borehole logs
41 with sufficient dating to correlate between datasets (Bridge, 2008).

42 Alluvial architecture can be considered at a variety of scales, from the bedform, barform, storey, channel
43 body, to system and finally to the basin scale (Fig. 1). Studies of alluvial architecture fall broadly into
44 three main scales, those that consider the internal geometry of sandstone bodies, those that consider
45 the external geometry of the sandstone bodies, which will be the focus of this study, and those that
46 consider the stratigraphic architecture of alluvial deposits (i.e. the stacking arrangement of the channel
47 bodies as addressed in the LAB model of Allen (1978), Leeder (1978) and Bridge and Leeder, (1979)), as
48 is demonstrated in Figure 1. These different scales are bound by a series of hierarchal surfaces as
49 described in Miall's (1988, 1996) architectural element analysis schemes, and demonstrated in Figure 1.
50 This study focuses on the geometry at the channel belt scale and below (i.e. the channel body scale).

51 Gibling (2006) discussed a range of studies that present alluvial architecture schemes that concentrate
52 on understanding the internal geometry and relationships of key surfaces and architectural elements
53 within a channel body. Examples include the schemes of Jackson (1975), Allen (1983), Miall (1985, 1996)
54 and Bridge (1993). The studies vary in terms of number of divisions present ranging from 3 (e.g.
55 microforms, mesoforms and macroforms of Jackson, 1975) to 8 different divisions (e.g. bounding
56 surfaces 1-8 of Miall, 1996), and generally vary in scale from the bedform to the channel body. However,
57 as is argued by Bridge (1993) they can be difficult to use due to the complexity of the schemes, or may
58 be oversimplifications in which important details are lost. Bridge (1993) also raises issues related to
59 restricted timescales of the different orders, and the fact that schemes do not account for how surfaces
60 may change order laterally. Despite the concerns raised by Bridge (1993), such schemes have been
61 widely applied in a variety of fluvial studies (e.g. Miall, 1988; Singh et al., 1993; Miall, 1994; Corbeanu et
62 al., 2001; Cain and Mountney, 2009; Leleu et al., 2009; Banham and Mountney, 2013; amongst others).

63 Gibling (2006) noted however that there are significantly fewer studies that comprehensively document
64 the external geometry (i.e. the overall geometry of sandstone bodies in three-dimensions) and
65 dimensions of fluvial deposits in the rock record. Examples of studies that consider and present schemes
66 of the external geometry of sandstone bodies include Friend et al., (1979, Fig. 1), Blakey and Gubitosa,
67 (1984, Fig 3), Hirst, (1991, Fig. 5), Gibling (2006, Fig. 4) Cain and Mountney (2009, Fig. 5), Huerta et al.,
68 (2011, Fig. 6), Pranter and Sommer (2011, Fig. 5), Gulliford et al., (2014, Fig. 5) and Owen et al., (2015a,
69 Fig. 3). However, from the range of schemes presented, it is clear that no single scheme has received
70 common acceptance, which may be the result of a lack of consistency related to differences in how
71 different schemes have been created (either width:thickness ratio, facies, or stacking arrangement
72 derived) or be related to differences in the range of scales at which studies have been conducted
73 (outcrop to partial basin).

74 Width: thickness ratios (e.g. 15:1) have been used to differentiate different geometries in previous
75 schemes, with further divisions being made based on 1) whether deposits are single or multistorey (e.g.
76 Friend et al. 1979, Blakey and Gubitosa, 1984, Hirst, 1991, and Huerta et al. 2011), or 2) were deposited
77 in confined and unconfined environments or form an amalgamated complex (e.g. Hirst, 1991). Huerta et
78 al. (2011) further subdivided sheet and ribbon geometries based on the degree of interconnectivity and
79 dominance of internal sedimentary features (accretions/bedforms). Pranter and Sommer (2011), used
80 numerical data as part of their scheme with absolute lateral extent measurements placed on the
81 different geometries, as opposed to width: thickness measurements and also, differentiated bodies

82   based on whether they were single storey, multistorey or formed large amalgamated channel
83   complexes. All other cited studies do not attach dimensions to their schemes, with Owen et al. (2015a)
84   considering only end-member geometries (single and multistorey bodies), Gulliford et al. (2014)
85   separating deposits at the sandstone body scale based on the nature of the stacking of channel belt
86   elements, and Cain and Mountney (2009) differentiating units based on whether deposits are
87   channelized or non-channelized elements, with further subdivisions based on facies present and
88   whether the fluvial channels were laterally stable or not.

89   It is important to recognise that the various studies were conducted over different spatial scales. With
90   the exception of Huerta et al., (2011), who studied a large portion of the Almazán Basin, Spain, the other
91   studies are restricted aerially to either single outcrop belts (e.g. Pranter and Sommer, 2011; Gulliford et
92   al., 2014), single depositional systems that are sourced from one catchment (e.g. Friend et al., 1979;
93   Hirst, 1991; Cain and Mountney, 2009; Owen et al., 2015a), or focus on a particular area of a basin (e.g.
94   Blakey and Gubitosa, 1984). The lack of consistency between the different studies and their general
95   limited aerial extent indicate that a basin scale comprehensive study on channel body architecture is
96   needed in order for channel body geometries from a range of systems (i.e. alluvial fan, distributive
97   fluvial systems/megafans or axial fluvial system) to be accounted for. This study therefore aims to begin
98   to address this problem by producing a classification scheme derived from a wide variety of fluvial
99   systems (i.e. differently sourced systems, as depicted in Figure 1) developed across a single sedimentary
100   basin.

101   **(2) Aims and methods**

102   This study focuses on documenting the internal and external geometries of channel bodies present
103   within the Palaeogene aged Fort Union and Willwood Formations of the Bighorn Basin, Wyoming (Fig.
104   2). Both Formations were studied, as paleocurrent maps presented by Seeland (1998) showed them to
105   be composed of the same genetic fluvial systems. Channel bodies are defined as a single, interconnected
106   mappable body of channel deposits – a definition modified from that of Potter (1967)(see Gibling, 2006
107   for discussion on terminology). The Bighorn Basin has excellent exposure across a considerable portion
108   of the basin fill, ensuring that this study can capture a wide range of fluvial architectures.

109   Sedimentological data in the form of sedimentary logs were collected that cover an area of 8,700 km^2,
110   and a total of 4,192 m of vertical succession, alongside architectural panels of the studied outcrops. A
111   total of 184 channel deposits were studied from 28 locations (Fig. 2), 12 from the Palaeocene Fort Union
112   Formation, 16 from the Eocene Willwood Formation,. Facies associations were depicted from
113   sedimentary log data in order to interpret depositional environments present. As is highlighted by
114   Bridge (1993, p.809) 'The geometry of an individual channel belt depends on the geometry of
115   channel(s), the mode of migration of the channels(s) within the channel belt and the rate of deposition
116   or erosion'. In order to capture these key processes, geometries within this study were defined based on
117   their internal characteristics (i.e. facies present, number of stories present and nature of internal
118   contacts) and external form to ensure that characteristics such as the mode of channel belt migration
119   and internal processes were documented. Storey surfaces are defiend in this paper to be erosional
120   elements of the active portion of a channel base, which incise into previous channel deposits, as is
121   shown in Figure 1. Storey surfaces therefore have associated bars and channel –fill deposits that filled
122   that particular incision event. These can either scale to one channel-fill (bar), or be associated with
123   multiple stacked bars. Widths cited in this paper are taken perpendicular to palaeocurrent flow.

(1) Geological setting

(2) Tectonic Framework and Basin Extent

The Bighorn Basin is situated in north-west Wyoming and south-central Montana (Fig. 2). It is a broadly NNW-SSE trending intermontane foreland basin that is 200 km long and 80 km wide (Willis and Behrensmeyer, 1995). The present basin margin is defined by the presence of several Laramide-age basement-cored uplifts (the Beartooth Mountains to the northwest, the Owl Creek Mountains to the south and the Bighorn Mountains to the east, Fig. 2), which formed as a result of the segmentation of the Late Jurassic to Cretaceous foreland basin of the western US due to a switch from thin- to thick-skinned deformation (Snyder et al., 1976; Dickinson et al., 1988; Decelles, 2004). The Pryor Mountains situated in the northern part of the basin close to the Wyoming-Montana border (Fig. 2) are also Laramide-age structures but are not thought to have been a continuous topographic barrier during the Palaeocene and Eocene (Kraus and Hasiotis, 2006). The southwestern part of the basin is currently largely overlain by the Absaroka Mountains (Fig. 2) which are composed of mid- to late-Eocene volcanic rocks (Rouse, 1937) and post-date deposition of the Fort Union and Willwood Formations. Several studies speculate the location of the southwestern margin of the Palaeocene-Eocene to be the Washakie Range (located approximately 30 km NE of Dubois, Wyoming), or the Cody Arch (Fig.2) (e.g. Kraus, 1985; Sundell, 1990; Lillegraven, 2009).

(2) Fort Union and Willwood Formations

The Fort Union and Willwood Formations were deposited in the Bighorn Basin during the Palaeocene and Eocene. A broad change in colour distinguishes the two formations, with the Fort Union Formation dominated by drab-grey palaeosols and the Willwood by lighter coloured red palaeosols (Willis and Behrensmeyer, 1995). The colour change has been attributed to either improved drainage as a result of reduced subsidence rates and continued high sedimentation rates (Gingerich, 1983), or due to a regional change to warmer and drier conditions (Willis and Behrensmeyer, 1995; and references within). A short lived (200,000 year), but abrupt warming (~ 5 °C) occurred at the end of the Palaeocene, known as the Palaeocene-Eocene Thermal Maximum (PETM) (Kennett and Stott, 1991; Kraus et al., 2015). This is recorded close to the boundary between the Fort Union and Willwood Formations, and has been extensively studied within the basin (e.g. Gingerich, 2003; Wing et al., 2005; Kraus and Riggins, 2007; Kraus et al., 2013; Wing and Currano, 2013; Foreman, 2014; Kraus et al., 2015).

The Palaeocene Fort Union Formation was deposited in a range of alluvial environments including alluvial fan, fluvial channels (braid plain and meandering), floodplain (e.g Kraus, 1985; Willis and Behrensmeyer, 1995; DeCelles et al., 1991 Seeland, 1998; Kraus and Hasiotis, 2006), and minor lacustrine deposits (e.g. Yuretich et al., 1984; Hickey and Yuretich, 1997). Palaeocurrent patterns from Seeland (1998), indicate rivers during the Palaeocene were flowing in a broadly north-east direction.

Deposits from the Willwood Formation also represent deposition from a suite of alluvial environments. Davies-Vollum and Kraus (2001), describe the Willwood Formation as mud-dominated with channel deposits representing deposition from sinuous rivers. Coarser grained deposits are intermittently present in the west which are interpreted to have been deposited in braid plains (Neasham and Vondra, 1972; Kraus, 1985). As a result of the excellent exposure of the floodplain deposits a suite of studies have focused on documenting the palaeosols of the Willwood Formation (e.g. Bown and Kraus, 1981; Bown and Kraus, 1987; Kraus, 1987; Kraus and Bown, 1993).

165   Despite the wide range of studies conducted on the Fort Union and Willwood Formations, only limited
166   work has focussed on describing the range of fluvial architectures present. Foreman (2014) (expanding
167   on the work of Kraus, 1980), presents the most detailed study on the internal architecture of channel
168   deposits, documenting the highly amalgamated nature of a sandstone complex that coincides with the
169   PETM. DeCelles et al. (1991) document the detailed internal architecture of the conglomerate deposits
170   in the northwest of the basin establishing seven orders of bounding surfaces within alluvial fan and braid
171   plain deposits. Kraus (1985) describes the internal structures found in conglomerates in the southwest
172   portion of the basin. Other studies have concentrated on documenting the fills of predominately mud-
173   filled avulsion deposits (e.g. Kraus, 1996; Kraus and Wells, 1999; Davies-Vollum and Kraus, 2001; Kraus
174   and Davies-Vollum, 2004), or present generic basin-scale alluvial architectural panels where channel
175   deposits are shown in relation to floodplain deposits (e.g. Fig. 3A of Kraus and Gwinn, 1997 and Fig. 2 of
176   Kraus, 2001). However, these studies are either of a limited aerial extent within the basin, or have
177   concentrated on a select few outcrops. The studies do, however, highlight that a range of alluvial
178   architectures are present within the basin-fill, and therefore there is suitable scope to present a basin
179   scale study of fluvial architecture.

180   **(1) Facies association description**

181   Two broad facies associations, fluvial channel and floodplain, have been identified.

182   **(2) Channel Facies Association**

183   Facies association descriptions in this section are concerned with describing sediments from the grain
184   scale up to, but not including, the storey scale (i.e. grain scale, bedform and barform scale, see Fig. 1).
185   Descriptions at the storey scale and above (i.e. the nature and cross-cutting relationships of stories) are
186   considered in the geometry section.

187   **(3) FA1 – Gravelly braided stream**

188   FA1 comprises conglomerates ranging from granule to boulder grade material with pebble to cobble
189   sized clasts predominating (Fig. 3A). The majority of clasts are very well-rounded quartzite and are
190   sometimes imbricated when a long axis is visible (Fig. 3A). Deposits are normally clast supported and
191   moderately sorted, but can on occasion be poorly sorted (Fig. 3A). Fining and coarsening up sequences
192   are often present over a 1-5 m scale. The matrix is composed of silt to coarse sand-sized grains. Thin
193   (0.5-4.3 m) wedge shaped sandstone packages can be present, but are not laterally extensive (< 25 m
194   wide) (Fig. 3C), and maybe internally structureless or display trough cross-bedding with a depositional
195   rather than erosional contact. Foresets (up to 4 m in height) which predominately dip in a downstream
196   direction, can on occasion be observed with lateral accretion surfaces only rarely identified. Horizontal
197   stratification can also on occasion be observed (Fig. 3B, C), making the deposits largely massive with
198   respect to the presence of bedforms and barforms

199   The largely massive nature of the deposits coupled with the presence of horizontal stratification and
200   minor presence of downstream accretion surfaces suggests bedload-sheet deposition, that in places are
201   indicative of longitudinal gravel bars through the presence of horizontal stratification and downstream
202   accretion surfaces (Rust, 1972). The wedge shaped sandstone packages are interpreted to represent
203   waning flow deposits on top of bar surfaces, on the channel floor, and/or accretion surfaces (Rust, 1972;
204   Ramos and Sopena, 1983). Kraus (1985) and DeCelles et al., (1991) describe similar deposits in the

205 Bighorn Basin and infer a braided depositional environment. Observations made in this study concur
206 with such interpretations as deposition from gravel sheets and dominance of downstream accretion
207 (when it can be observed) and a generally low spread in palaeocurrent direction (Fig. 3A) are more
208 diagnostic of braided environments (Bristow and Best, 1993) and largely absent from meandering
209 systems.

(3) FA2 – Heterolithic, dominantly braided

211 FA2 includes a range of grain sizes from medium sandstone to cobble sized clasts with sandstone
212 forming approximately 30% of the facies association and conglomerate 70%. Sedimentary structures
213 such as horizontal lamination and trough cross-bedding are more commonly observed in FA2 in
214 comparison to FA1, with sets rarely reaching 1 m in thickness. Granule sized grains often line trough
215 cross-laminae surfaces (Fig. 4A). Conglomerate deposits in the north-west of the basin are generally
216 more rounded and better sorted than those in the south-west where clasts are more angular and matrix
217 supported (Fig. 4B). Accretion surfaces are more prevalent than in FA1, with downstream accretion
218 surfaces, up to a maximum of 6 m in thickness, being more prevalent than lateral accretion surfaces (Fig.
219 4C).

220 The presence of bedforms and barforms throughout the deposits suggests more sustained flow
221 conditions, in which sediment load may have been reduced in comparison to FA1, allowing bedforms to
222 develop. The deposits are regarded to be from mixed braided-meandering planform (i.e. a wandering
223 planform), with the former dominating as is indicated by the dominance of downstream relative to
224 lateral accretion surfaces and relatively low spread in paleocurrent directions (Fig. 4C). The mixture of
225 the two grainsizes (Fig. 4) suggests deposition either in proximal environments where textural sorting is
226 not yet achieved, or that a flashy discharge regime was present .

(3) FA3 – Heterolithic dominantly meandering

228 The deposits of FA3 are composed predominantly of fine to medium sand, but can range from silt to
229 coarse sand. Granules, carbonate nodules and mudclasts may line trough cross-sets, accretion surfaces,
230 and form lags at the base of storey surfaces (Fig 5A). Mud may also be present as part of heterolithic
231 accretion packages (Fig. 5B) or as scour fills. The sediments are generally well sorted, with grains ranging
232 from sub-angular to sub-rounded. Trough cross-bedding is the dominant structure (Fig. 5A, C) with
233 upper-plane-bed lamination also common. Current ripples, lower plane bedding, and soft sediment
234 deformation (Fig. 5D) form minor constituents of the deposits. Thin, organic-rich layers containing fossil
235 leaves may be present at the base of channels, or line accretion surfaces, but such deposits are only
236 found associated with poorly drained sequences (see palaeosol descriptions). Lateral accretion is more
237 prevalent than downstream accretion, and accretion packages can either be heterolithic or composed
238 entirely of sand. FA3 is predominantly composed of multiple bar deposits (Fig. 5B), but channel fills in
239 which only a single bar deposit (which can reach thickness of 6 m) can on occasion be observed.

240 The moderate sorting of material suggests deposition from relatively perennial flow conditions, with the
241 presence of coarser grains, mud clasts and carbonate nodules on cross-sets indicating fluctuations in
242 discharge. The prevalence of lateral accretion which is found alongside downstream accretion suggests a
243 wandering planform in which a meandering form prevailed, but also contained braided features (i.e.
244 mid-channel bars). A higher spread in paleocurrent data supports this interpretation, as can be seen in
245 Figure 5B. Sand-dominated channel deposits have also been recognised in the basin by other authors,

246 such as Kraus, (1987), Willis and Behrensmeyer (1995), Kraus (1996), Kraus and Wells (1999), Kraus
247 (2001), Jones and Hajek (2007), and Foreman (2014).

(3) FA4 – Fine grained channel fill

249 The grain size of facies association FA4 ranges from silt to medium sand. Current ripples and trough
250 cross-bedding can be found in sand grade material, while horizontal lamination can be observed in both
251 mud and sand grade beds. The deposits of FA4 are relatively simple in nature. Accretion surfaces are
252 very rare, while multiple small scale (<1 m) horizontal beds (Fig. 6A), that can either be heterolithic in
253 nature or entirely composed of mudstones (Fig. 6B), are common. Pedogenic modification (rootlets and
254 mottling) can on occasion be observed.

255 It is hypothesised that the mud-dominated channels are either abandoned channel fills (e.g. Hornung
256 and Aigner, 1999; Kraus and Davies-Vollum, 2004), or were groundwater fed channels (e.g. Singh et al.,
257 1993). In the case of the heterolithic bedded fills, the channels are interpreted to have been deposited
258 from rivers with intermittent, lower discharges, possibly in distributary channels or proximal splay
259 environments (Banham and Mountney, 2013).

(2) Floodplain Facies Associations

261 Due to the extensive exposure of floodplain deposits in the Bighorn Basin there have been numerous
262 studies that document their characteristics (e.g. Bown and Kraus, 1981; Yuretich et al., 1984; Bown and
263 Kraus, 1987; Kraus, 1987; Kraus and Bown, 1993; Hickey and Yuretich, 1997; Kraus and Gwinn, 1997;
264 Davies-vollum and Wing, 1998; Kraus and Hasiotis, 2006; Abdul et al., 2008; Abels et al., 2013). As this
265 paper focuses on channel deposits in the basin, floodplain characteristics are only briefly described.
266 Three elements were recognised: lacustrine, palaeosol, and splay deposits.

(3) FA5 - Lacustrine

268 Lacustrine deposits were only documented in the northern portion of the basin at location 14 (Fig. 2).
269 Deposits can either be mud- or sand-dominated, contain horizontal stratification (Fig. 7A) and
270 bioturbation, with trough cross-bedding (<50 cm) and current ripple lamination forming only minor
271 constituents of the beds when sand fractions dominate. The sandstone deposits have sharp bases and
272 have a tabular form (Fig. 7B). Mudstone deposits are clay to silt grade, have a drab grey colouration and
273 are horizontally laminated (Fig. 7A). Only one limestone bed was measured in the basin in this study but
274 this lithology has been documented by Yuretich et al. (1984) and Hickey and Yuretich (1997) in the
275 northern portion of the basin. The limestone bed was composed of lime mud, where faint wavy to
276 horizontal lamination and one gastropod were observed. The lacustrine deposits are often closely
277 associated with thin (< 50cm thick) beds of coals (Fig. 7B). The lacustrine deposits are not considered to
278 have been deposited in large lakes, but rather from shallow, aerially restricted lakes that were likely
279 subtle topographic depressions on the floodplain (Yuretich et al., 1984; Hickey and Yuretich, 1997).

(3) FA6 - Palaeosols

281 Palaeosol deposits have received a considerable amount of attention in the Bighorn Basin, particularly
282 with regards to the Palaeocene Eocene Thermal Maximum (e.g. Kraus et al., 2015). Comprehensive
283 descriptions of palaeosols present within the basin include Bown and Kraus (1981), Bown and Kraus
284 (1987), Kraus (1987), Kraus and Bown (1993), Kraus (1999), Kraus and Hasiotis (2006), Kraus and Riggins

285 (2007), and Kraus et al. (2015). Two broad types of palaeosols are defined across the entire basin
286 namely moderate to well-drained palaeosols and poorly-drained palaeosols.

287 The moderate to well-drained palaeosols range in grain size from clay to fine-medium sand, with sandy
288 silt dominating. Individual rootlets, rhizoliths, carbonate nodules, slickensides, mottling (purple, orange,
289 and red), organic matter, and bioturbation are all observed to varying degrees in the well-drained
290 palaeosol sequences, while primary features are very rarely observed (Fig. 7C, D). The well-drained
291 palaeosols are generally moderately to well-formed cumulative soils and are various shades of red in
292 colour (Fig. 7C), indicating oxidation of the soils (Retallack, 2001). The well-drained palaeosols are most
293 dominant in the Willwood Formation, but do also occur in the Fort Union Formation.

294 Poorly-drained palaeosols also range from clay to fine-medium sand in grain size, with sandy-silt grain
295 sizes dominating. The poorly-drained palaeosols also contain rootles, slickensides, mottling (orange,
296 purple, and red), and burrows but to a lesser degree than that of the well-drained palaeosols with the
297 exception of organic matter which is more prevalent in the poorly-drained facies. In addition, yellow-
298 brown accumulations are also observed, and represent goethite deposits (Kraus and Hasiotis, 2006). The
299 poorly-drained soils are less mature than the well-drained soils, and possess a grey, dark grey, green-
300 grey, and purple colouration (Fig. 7D). These characteristics suggest the soils were relatively saturated,
301 which could either be due to high water tables, or due to the characteristics of the soil hindering
302 drainage (i.e. grain size) (Kraus, 1999). Thin, organic rich carbonaceous layers and thin coals (<1m) are
303 associated with the poorly drained soils, but are relatively uncommon across the basin. Poorly drained
304 soils are present across the basin, but are more prevalent in the Fort Union Formation on the periphery
305 of the basin, and in the northern portion in the basin centre.

306 **(3) FA7 - Splay and sheet flood deposits**

307 Sheet and ribbon sandstone deposits form common constituents of floodplain material in the Bighorn
308 Basin. The grain size ranges from very fine sand to coarse sand in sheet sandstones, with sediments
309 generally well sorted with floating granules rarely present. Horizontal lamination, ripple lamination and
310 trough cross-bedding are all present. Vertical, horizontal, and sub-horizontal burrows are observed to
311 varying degrees. The sheet sandstones are interpreted to represent unconfined flow conditions on the
312 floodplain, either as part of a splay complex (terminal or lateral e.g. Fisher et al., 2007), or may have
313 formed from overtopping of the banks of the channel (e.g. Shen et al., 2015).

314 The ribbon sandstones (as defined by Friend, 1983) are composed of a single fill of trough cross-bedding,
315 ripple lamination and horizontal lamination, and do not contain any bars. Based on their internal
316 characteristics and intercalative relationship with sheet sandstones and paleosols, these channels are
317 interpreted to be the channelized portion of splay deposits, and have also been noted in previous
318 studies (e.g. Kraus, 1987; Kraus, 1996b; Kraus and Wells, 1999; and Kraus and Davies-Vollum, 2004).

319 **(1) Sandstone body geometries**

320 Seven sandstone body geometries are defined within this study; five of which are associated with
321 channel facies, which is the focus of this study, and two of which are associated with floodplain facies
322 (Fig. 8). The five channel geometries are defined based on overall geometric shape and internal
323 relationship of storey surfaces. Here the geometries present are described, with potential controls on

324   the different geometries presented in the discussion section. Summary information can be found in
325   Table 1.

(2) M – Massive channel body geometry

327   The massive channel body geometry has a wide range of thicknesses measured (n=8), ranging in
328   thickness from 5.7 – 47.5 m (Fig. 9). Due to its large size, full lateral extents cannot often be measured;
329   however at Location 16 (Fig. 2, Fig. 10A), a lateral extent of 5.5 km was observed. The deposits pinch out
330   laterally into floodplain material, defining a large, broad channel geometry. Minimum lateral extents did
331   not exceed 1.5 km, however these measurements were the result of exposure limitations. There is
332   commonly little relief on the basal incision surface (up to 3m) when compared to the size of the bodies
333   (up to 47.5 m), with both convex and concave geometries observed (Fig. 8A, Fig. 10A)

334   Internally, the deposits are considered to be massive with respect to the lack of apparent storey
335   surfaces present, which is a defining internal feature of this geometry. Storey surfaces are rare, but
336   when present up to five storey surfaces can be observed (average of 2.1 stories present), which have
337   thicknesses ranging from 1.4 – 47.5 m (average of 10.1 m). Storey surfaces have limited lateral (up to
338   200 m) and vertical relief (2 m), and therefore do not appropriately scale to the size of the channel body
339   (Fig. 10A). The storey surfaces do not cross-cut one another and transition into sediments laterally
340   ('transitional surface' in Fig. 8A). It is speculated that the coarse grain size makes identifying storey
341   surfaces difficult, and it is therefore not ruled out that many more may be present. M can be composed
342   of FA1 and FA2 and is considered to be similar to the sheet-like channel bodies with high
343   interconnectivity of Huerta et al. (2011). It can be inferred that geometry M can be applied to some of
344   the deposits previously described within the basin by Kraus, (1985) and Decelles (1991) based on images
345   and descriptions within the texts.

(2) SA - Semi-amalgamated channel body geometry

347   The semi-amalgamated channel body geometry (SA) has an external geometry in which broad sheet-like
348   bodies are semi-amalgamated, with up to 50% of the channel belt base in contact with floodplain
349   deposits and the remainder with a channel deposit on channel deposit contact (i.e. transitions into a
350   storey surface) (see Fig. 8B for diagrammatic explanation, Fig. 10B for example). This results in a semi-
351   amalgamated irregular external form which has pockets of floodplain material that locally separate
352   channel deposits along the margins of the body (Fig. 8B, Fig. 10B). Paleocurrent directions were found to
353   be relatively consistent between the amalgamating portions, supporting the notion that the
354   amalgamation is not a local feature, indicating that a complex three-dimensional geometry is present. As
355   with M, the extremities of the deposits were only rarely observed and when done so the deposits pinch
356   out laterally into floodplain deposits. Channel bodies with a SA geometry range in thickness from 1 –
357   44.5 m (N= 42) (Fig. 9), with an average of 7.5 m calculated, with the largest minimum lateral extent
358   measured as being 3.5 km.

359   Internally, storey surfaces are more prevalent than in geometry M. Storey surfaces can be both spatially
360   isolated from one-another, or can cross-cut one another (Fig. 8B, Fig. 10B). SA is considered to be
361   predominantly multistorey with up to three storey surfaces identified (average of 1.3 stories present,
362   Table1) within a single SA body. Individual story packages range in thickness from 1- 30.3 m (average
363   thickness 5.7 m), although again issues with exposure quality in the latter may be yielding apparent
364   thicknesses. Geometry SA can be composed of FA1, FA2 and FA3. It is considered to be geometrically

365 similar to complex type B of Gulliford et al., (2014). As with geometry M, it can be inferred from
366 descriptions and images within Kraus, (1985) and Decelles (1991) that Geometry SA can be allocated to
367 some of the deposits described within the recognised studies texts.

(2) IA – Internally amalgamated channel sheet geometry

369 Geometry IA has a simpler form than SA with a broadly sheet-like form (Fig. 8C, Fig. 10C) that extends
370 laterally for up to 3 km's in Willwood exposures, however it is suspected this is a minimum due to
371 outcrop limitation. The channel geometry is simpler and more uniform in nature than that of SA (Fig. 9).
372 When visible the deposits pass laterally into floodplain deposits in a gradational manner, but on
373 occasion a steep cut bank can be observed. IA ranges in thickness from 4.1 m to 27.6 m (N= 46) (Fig. 9),
374 with an average of 11 m calculated.

375 Internally, IA generally has the most abundant storey surfaces present of all the geometries described
376 (average of 2.4 stories, Table 1) IA is multi-storey with 2 to 4 stories present (Fig. 10D). Storey surfaces
377 can be laterally extensive (up to 300 m measured) but are most commonly truncated laterally and
378 vertically by other storey surfaces (Fig. 8C, Fig. 10D). Transitional storey surfaces, where storey surfaces
379 laterally taper out and become indistinguishable, are on occasion observed ('transitional storey' in Fig.
380 8C). Storey packages are on average 4.6 m thick, ranging from 1.5 m to 14.3 m. IA can be composed of
381 FA2, but more commonly FA3 and FA4. IA is recognised in many schemes including the multistorey sheet
382 of Blakey and Gubitosa (1984), multistorey/multilateral and amalgamated complex of Hirst (1991) and
383 Pranter and Sommer (2011), the amalgamated channel-fill complex of Cain and Mountney (2009), the
384 intermediate sheet-like bodies of (Huerta et al., 2011), and the amalgamated channel belt of Owen et al.
385 (2015a). Geometry IA has been recognised as sheet sandbodies in other studies conducted in the
386 Bighorn Basin such as Kraus and Middleton (1987), Kraus (1996), Davies-Vollum and Kraus (2001), Kraus
387 and Davies-Vollum (2004) and Foreman (2014).

(2) OS - Offset stacked channel body geometry

389 The internal arrangement of storey surfaces distinguishes geometry OS from IA. In OS, storey packages
390 are juxtaposed onto one another in an offset manner laterally and vertically, resulting in some surfaces
391 being in contact with underlying channel deposits, and others in contact with underlying floodplain
392 deposits (Fig. 8D). In this respect, OS can be either single storey or multistorey depending on where it is
393 defined (Fig. 11A), with 1 to 3 stories present (average of 2 stories present, Table 1), that range in
394 thickness from 0.3 to 7.1 m (average of 3.8 m). This results in a complex irregular external sheet like
395 geometry (Fig. 8D, Fig. 11B). Internally the deposits are composed of offset stacked channel-fill deposits
396 with only partial vertical juxtaposition, resulting in limited lateral and vertical connectivity and high
397 spatial variability in thicknesses across channel bodies (Fig. 8D, Fig. 11A). The minor but important
398 vertical juxtaposition can result in a subtle climbing trajectory of the deposits. Offset stacked sheet
399 sandstones range in thickness from 2.4 m, when measured at a point in which only a single storey is
400 present, to 13.7 m in thickness when several stories are amalgamated (average of 7.7 m calculated,
401 N=12) (Fig. 9). When compared to M, SA and IA, OS has a relatively narrower range in thicknesses (Fig.
402 9). Exposure limitations meant that a maximum lateral extent could not be obtained, however the
403 largest lateral extent measured was 1 km. OS can be composed of FA3 and FA4. To the authors
404 knowledge this geometry has not been previously documented in the Bighorn Basin, and has only been
405 previously recognised in Gulliford et al. (2014) as their complex type A.

(2) I - Isolated channel body geometry

The isolated channel body geometry (I) is single storey, with no internal storey surfaces present (Fig. 8E) and is composed of FA3 and FA4. I is considered to possess a simple 'classic' external channel geometry, which can either be asymmetric when only a steep cut bank is observed on one side (Fig. 11C), or symmetric when it is observed on both sides of the channel body (Fig. 8E). Channel bodies do not extend laterally for more than 1 km, and has the smallest range in thicknesses of the geometries, ranging from 1.7 m to 11.4 m (average of 4.2 m calculated, N=76) (Fig. 9). The isolated channel body geometry is recognised in all cited schemes (Friend et al., 1979; Blakey and Gubitosa, 1984; Hirst, 1991; Cain and Mountney, 2009; Huerta et al., 2011; Pranter and Sommer 2011; Gulliford et al., 2014; and Owen et al., 2015a), but may be reffered to as ribbon, fixed or single storey channel bodies (i.e. width-to-thickness aspect ratio of 15:1, Friend et al., 1979). It has also been regonised as ribbon geometries in Kraus and Middleton (1987), Kraus, (1996), Davies-Vollum and Kraus (2001)and Kraus and Davies-Vollum (2004).

(2) Floodplain sandstone geometries

Two sandstone geometries were observed within the floodplain facies association; sheet (FS) and ribbon channel (FR). Sheet sandstones generally have a tabular form with sharp bases (Fig. 7D, 8F), but undulating forms are also present. When observed, sheets pinch-out laterally over large distances (up to 1 km observed), and do not exceed more than 2 m in thickness. This results in the sheets possessing a very broad concave-down geometry. Ribbon sandstones range in thickness from 0.2 to 3.4 m (Fig. 7E, 8G) (1.2 m average), are not laterally extensive (<150 m wide), and possess a similar geometric form to the channel geometry I.

(1) Discussion

A sandstone body geometry scheme has been presented based on a basin wide study from the Bighorn Basin, Wyoming. A total of seven different sandstone geometries have been defined from channel and floodplain facies. To the authors' knowledge this is the first study to document a suite of channel geometries across a near entire depositional basin. As a result, a wider array of channel body architectures has been captured in comparison to previous studies within the Bighorn Basin and beyond, which are summarised in Figure 8. It is recognised that Gibling (2006) complied a scheme from a large literature based dataset, however our study is able to put the described sandstone geometries in context of one another as well as describe key internal characteristics (facies present and storey surface characteristics) to help devise the scheme. It is considered that the scheme presented in this paper has subdivided the 'sandstone sheet' geometry used in many classification schemes (e.g. Friend et al. 1979) into 4 distinct geometries (M, SA, IA, OS) based on the internal arrangement and nature of storey surfaces which reflect processes that formed the sandstone bodies rather than just width: thickness data being the diagnostic feature. Other studies such as Hirst (1991) do recognise the multistorey nature of described sheet sandstones, which has now been built upon. The ribbon geometry has also been recognised (I) as well as two sandstone body geometries (FS and FR) within the floodplain facies association.

(2) Controlling factors

A key defining feature of the different sandstone geometry types in Figure 8 is the nature and stacking style of the storey packages. There is also an apparent relationship with regards to sandstone geometry

446 and facies associations present (i.e. grain size and sorting, nature of bar deposits), with certain facies
447 associations only being found within certain sandstone body geometries. These factors therefore may
448 give potential insights into what the key controls on determining the different sandstone body
449 geometries are. Traditional models that assess fluvial architecture, such as the LAB model (of Leeder,
450 1978, Allen, 1978, and Bridge and Leeder, 1979), consider amongst other things such as compaction,
451 and tectonic movement on floodplain margins, that sedimentation rate, aggradation rate and channel
452 belt avulsion frequency have a profound effect on the formation of different fluvial stacking styles. From
453 a simple perspective, when all other parameters are considered constant, reduced sedimentation rates
454 result in a high stacking frequency of channel deposits, and high sedimentation rates result in a low
455 stacking frequency of channel deposits (e.g. Bridge and Leeder, 1979). Whilst most studies that take this
456 approach are largely focussed at the stratigraphic architecture scale (see Fig. 1), the same principles can
457 be applied at the storey scale when considering the stacking arrangement of storey packages. This study
458 therefore considers processes that occur over approximately a 10^0-10^4 years scale (after Miall, 2016).
459 Each of the channel body geometries identified here are discussed in this context such that a
460 comparison can be drawn between them.

461 Internally, geometry M possesses a limited amount of storey surfaces that do not cross-cut one another,
462 which have minimum lateral extents (200 m max) and erosional relief (2 m) (Table 1, fig. 8). Their limited
463 lateral extent is interpreted to represent either; 1) brief incision phases that were not sustained in
464 strength or time; or 2) indicate that there was insufficient grain size contrast to distinguish further
465 surfaces. If the former interpretation is correct, then this suggests minimal deposit reworking which is
466 consequence of high aggradation and sedimentation rates or static discharges. Evidence for high
467 sediment supply and storage can be seen by the dominance of FA1 and FA2 in geometry M which are
468 interpreted as gravel braid sheets. However, if it is inferred that more storey surfaces are present, a low
469 accommodation to sediment supply regime can be considered, in which the channels were highly
470 mobile, which the braided interpretation with a coarse grain and limited low relief barform presence
471 would support.

472 Geometry SA has a higher abundance and larger lateral extent of storey surfaces relative to geometry M
473 suggesting higher rates of channel migration and reworking. A higher dominance of FA2 (better sorting
474 and reduced grain size), suggests a reduced sediment supply in comparison to M. However, SA is still
475 considered to have a relatively high sediment load, as indicated by the poorly sorted nature (indicating
476 relatively proximal locations where sediment supply is deemed to be highest), the subdued nature of
477 the bedforms and barforms, and presence of FA1 and 2 with intercalations of FA3. Geometry SA reflects
478 an aggradation rate that is not sufficient enough toelevate subsequent channel deposits above the
479 floodplain, with basal storey surfaces removing floodplain material resulting in juxtaposition against
480 underlying channel body deposits. The preservation of some floodplain (that separates channels in some
481 areas), is deemed to be due to incision not being extensive across the channel belt area. This results in
482 an irregular geometry in which minor, non-continuous floodplain remnants are preserved (Fig. 8B, 10B).

483 A high degree of reworking and juxtaposition of storey surfaces is also evident in geometry IA as shown
484 by the cross-cutting nature, abundance of, and more continuous extent of, storey surfaces. However key
485 differences between geometry IA and SA are the more distinctive tabular form of IA and lack of
486 floodplain intercalations. A lack of floodplain intercalations suggests two scenarios with respect to
487 aggradation rates: 1) following channel avulsion floodplain aggradation was sufficient to separate and
488 define the distinctive IA sheet geometry rather than amalgamate to form a SA geometry or, 2) the rate

489   of reworking was too high to allow floodplain deposits to be preserved. The dominance of FA3 and FA4
490   suggests there was reduced sedimentation in comparison to M and SA, as bedforms and barforms are
491   more abundant and pronounced, and sediment is generally better sorted (Collinson, 1996). The
492   intermittent presence of FA2 does suggest a fluctuating discharge. These factors favour scenario 1 in
493   which relatively high floodplain aggradation rates were present as the decrease in lateral extents,
494   thickness and storey height relative to geometry SA (Table 1) implies the channels were smaller in size
495   such that it is difficult to envisage such small scale channels creating such large scale reworking The
496   channels are considered to have been deposited from a sinuous planform, as is suggested by the
497   dominance of FA3 and 4 in which lateral accretion deposits dominate. Storeys are observed to either
498   systematically migrate across the channel belt, as shown by the lateral migration of storey packages, or
499   occur randomly juxtaposed onto previous deposits with little evidence for lateral migration of the
500   channel belt, possibly resulting from intra-channel belt avulsion of the active channel.

501   A relative difference in aggradation rate is also considered to have produced geometry OS. Higher
502   aggradation rates resulted in an important lateral and vertical migration of the channel where the
503   channel 'steps' along the landscape in a subtle climbing trajectory (as depicted in fig. 8D), or when
504   elevation of the floodplain is sufficient for channel emplacement (avulsion) to occur in a random
505   manner. This results in a lower degree of amalgamation of storey packages in geometry OS relative to
506   IA, with storey packages only partially amalgamating with one another to produce an irregular tabular
507   body at a larger scale (fig. 11B). Geometry I shows no evidence for reworking at the storey scale as no
508   storey surfaces are defined. This indicates that the river was relatively fixed in position, and that there
509   was channel migration through avulsion in a setting in which there was ample aggradation and space for
510   it to do so and not juxtapose onto previous deposits. The dominance of FA4 and moderate identification
511   of FA3 for geometry I implies reduced sedimentation rates as indicated by the better sorting of sediment
512   (Collinson, 1996) and clearly defined bar features and bedforms in comparison to all other geometries.

513   It is therefore considered that a combination of degree of channel migration, aggradation rate and
514   sediment load to vary between the described geometries and to form the key controls on geometry
515   development. Such controls have also been noted by Bristow and Best (1993) to be key in the
516   preservation of braided morphology (Fig. 5 of Bristow and Best, 1993) and also in Figure 15 of Gibling
517   (2006). The relative differences between the different geometries could be the result of changes in the
518   accommodation and sediment supply regime through time. The changes in sediment supply and
519   accommodation can occur over two different scales; at the longer allogenic or shorter autocyclic scale.
520   However as discussed by Cecil (2003) these two scales can overlap. Large scale regional and detailed
521   mapping is needed to capture both scales, as has been done in on fluvial systems studied by
522   Rittersbacher et al., (2014) and Owen et al., (2015b). Autocyclic changes are deemed to be relatively
523   local in nature resulting in minor discontinuities (Miall, 2016). Unless surfaces are able to be mapped
524   regionally, which the cases described in here were not able to be, it is deemed that the storey surfaces
525   and subsequent fills were largely under the autocyclic scale control (e.g. local storage and release of
526   sediment, seasonal fluctuations in discharge). However, longer term allocyclic controls (i.e. tectonics and
527   climate) will also have an overriding background influence on this (i.e. sediment delivery to basin which
528   can be controlled by climate and tectonics, Cecil, 2003). Longer term controls will eventually lead to the
529   different stacking patterns of the storey surfaces seen in the different geometries. The different
530   geometries can therefore provide information on the local variations in accommodation and sediment
531   supply. It is speculated that the repeated stacking of certain geometries will help infer allocyclic trends.

532   For example, a high accommodation and low sediment supply regimes may be dominated by geometries
533   OS and I, while a low accommodation and relatively high sediment supply regime may be dominated by
534   geometries M and SA. However, this scale is deemed outside the scope and scale of this paper, and
535   further stratigraphic scale (Fig. 1) analyses would be needed.

536   Even when all parameters are considered static, changes in sediment supply and accommodation could
537   also be related to downstream changes in proximity from the mountain front to the basin centre, as is
538   seen on distributive fluvial systems (DFS) (e.g. Nichols and Fisher, 2007; Weissmann et al., 2010;
539   Weissmann et al., 2013; Owen et al., 2015a; Weissmann et al., 2015), or a combination of the two. It is
540   infered that the presented geometries are present along a continuum, with the five geometries
541   identified representing key transitional geometries along that continuum. Figure 12A, shows the relative
542   percentage that each channel geometry comprises the total channel deposits at each location studied.
543   Evidence for the geometries being along a continuum can be inferred when looking at the general
544   trends. Geometry M and SA dominate the peripheries of the basin (proximal regions). Geometry IA can
545   be observed in both the basin margin and basin centre and do not appear to be preferentially situated in
546   any part of the basin. Geometry OS is dominantly found in the basin centre, and while I is present across
547   the basin it dominates the interpreted basin centre (distal regions). Although trends are masked by
548   inherent variability that is inevitably present when multiple systems compose a sedimentary basin fill,
549   the general trends do suggest there is a spatial control on geometry presence from basin margin to the
550   interpreted basin centre and therefore the geometries can be inferred to be along a continuum (Fig
551   12b). Further evidence for the deposits lying along a continuum can be found in Table 1 where a
552   decrease in maximum lateral extents, storey thickness, and a change in the facies associations that
553   dominate from geometry M through to I are seen. Although the maximum thickness of the channel fill
554   bodies does generally decrease (Table 1), it is not observed in the average thickness, which may be the
555   result of differing sized channels or systems within the basin. Evidence for the geometries being along a
556   continuum was also found in a down depositional dip section where M transitions into SA. It is therefore
557   speculated that IA represents the disarticulation of SA, with further disarticulation causing the individual
558   storey complexes to become only partially connected in an offset manner (OS), until finally transitioning
559   to geometry I, as is depicted in Figure 12B. A note does need to be made on the age of the deposits as
560   the deposits become progressively younger towards the centre of the basin due to its synclinal form
561   (Fig. 12A). Preliminary data presented in Figure 12A, does indicate that no geometry is associated with
562   any particular age group, suggesting there is no temporal control (and therefore possible allocyclic
563   control) on geometry formation at the channel body scale. A full temporal analyses would however need
564   to be conducted to fully assess this, which is out of the scope of this study. It is also important to
565   recognise that the age of the deposits at each particular location as other geometries may be found
566   higher, or lower, in the stratigraphy at the same locations. It is emphasised here that the interpretations
567   above are speculative and that high resolution aggradation rates and/or improved modelling efforts are
568   required to better constrain the key controls on channel body geometries.

569

570   (2) **Wider applicability**

571   It is speculated that the geometries observed in the Bighorn Basin may be able to be observed in other
572   sedimentary basins in which fluvial deposits reside. Figure 13 documents an example of each geometry
573   from different formations across the globe, with geometry M being observed in the Altos de Pica

574 Formation, Chile (Fig. 13A), geometry SA in the Sariñena Formation, Spain (Fig. 13B), geometry IA in the
575 Morrison Formation, Colorado (Fig.13C), geometry OS also from the Sariñena Formation, Spain (Fig.
576 13D) and geometry I from the Chinle Formation, Utah. However, further documentation from several
577 other basins is required before this is apparent. It is acknowledged that the facies, sediment calibre,
578 architectural elements, or the scale of the geometries described may differ from basin to basin in
579 relation to variation in the size of systems and source terrains. As a result facies, or quantified data in
580 these forms, has not been included in the classification scheme (Fig. 8). A width: thickness ratio has not
581 been added as firstly; exposures of full lateral extents and thicknesses are not commonly able to be
582 gained in many outcrops and secondly; there is also considerable overlap between width: thickness
583 ratios (see Table 1 and Figure 9, and Gibling, 2006), raising questions to its applicability in defining
584 sandstone body geometry (see Bridge and Tye, 2000). Although it is not suggested that a specific size of
585 body should be related directly to a particular sandstone geometry, it is recognised that some
586 geometries (i.e. IA) are generally larger than others (i.e. I). It is recognised that geometry identification
587 will be difficult in outcrops of limited lateral extent and in the subsurface. However, the geometry-based
588 architectural scheme presented here together with the description of the internal relationship and
589 nature of the storey surfaces along with facies descriptions may aid identification of the described
590 geometries in poorer quality outcrops.

591 **(1) Conclusions**

592 This study presents the results of a basin wide architecture study of Palaeocene to Early Eocene aged
593 fluvial deposits in the Bighorn Basin, Wyoming. Key facies associations from channel and floodplain
594 environments have been described with the commonly used sheet sandstone geometry further
595 classified into 4 sub-geometries (Massive structureless channel body geometry (M), Semi-amalgamated
596 channel body geometry (SA), Internally amalgamated channel body sheet geometry (IA) and Offset
597 stacked channel body geometry (OS)) with an Isolated channel body geometry (I)) also being defined,
598 The different geometries have been defined based on external geometric form and internal
599 arrangement and nature of storey contacts. It is hypothesised that the different geometries are part of a
600 continuum of fluvial channel geometries present in the depositional record. The stacking rate and style
601 is deemed to be a key controlling factor, which is related to degree of channel migration which has been
602 speculated to be related to sediment supply and accommodation available. Two floodplain geometries
603 (sheet and ribbon) are also described. This study highlights the range of channel body architectures that
604 may be present in continental sedimentary basin fills.

605 **(1) Acknowledgements**

612 **FIGURES**

613   1) Scheme of the different hierarchical scales at which fluvial architecture can be considered and how
614   they may vary in both time and space at the different scales. This study concentrates on understanding
615   the geometry of fluvial deposits at the channel body scale.

616   2) Location map of the study area. See text for references to location numbers cited.

617   3) Example images of Facies Association 1; A) Note the well-rounded nature and clast supported nature
618   of the conglomerate deposits. Note the consistent imbrication direction in rose diagram. Image taken at
619   Location 16; B) Example of horizontal stratification taken from Location 1; C) Interpreted photo showing
620   the subtle accretion surfaces and horizontal stratification found in Facies Association 1 at Location 16.
621   Note the sandstone packages are not laterally extensive and occur as small pockets within the
622   conglomerates and lack of continuity of storey surfaces.

623   4) Example images of Facies Association 2 taken from Location 27; A) Image demonstrating the poorly
624   sorted nature that is common in Facies Association 2 with large clasts lining trough sets; B) Example of
625   an immature texture from fine grained conglomerate deposits found in the facies association; C)
626   Example of accretion packages that are more commonly seen in Facies Association 2 in comparison to
627   Fig. 3. Rose diagram depicts cross-bedding direction for outcrop shown.

628   5) Example images of Facies Association 3; A) Image demonstrating the poorly sorted nature that can be
629   observed in the facies association. Note that a range of material (mudclast, nodules and pebbles) can
630   line trough sets. Pencil for scale. Picture taken from near location 25; B) Example image of heterolithic
631   accretion surfaces from Location 12. Rose diagram uses cross-bedding direction measurements note the
632   high variability; C) Example of the large scale clean cross-bedded unit from Location 7; D) Example image
633   of soft-sediment deformation commonly observed in Facies Association 3 taken from Location 22.

634   6) Example images of Facies Association 4; A) Example of the planar bedded fill within a channel deposit
635   from Location 26. Internally, beds are composed of small scale trough-cross beds, planar and ripple
636   lamination; B) Example of a mud-fill channel deposit from Location 15.

637   7) Example images of floodplain Facies association found in the Basin; A) Example of sandstone deposits
638   fond in the lacustrine facies at Location 14. Note the sharp base and lateral continuity; B) Example of a
639   lacustrine dominated section with associated coal deposits from Location 14; C) Moderate- to well-
640   drained palaeosol deposits intercalated with sandstone sheets. Mottling and rooting are common
641   features within this palaeosol type. Image from Location 18. D) Poorly-drained palaeosol deposits which
642   are commonly closely associated with sheet sandstone deposits from Location 6; E) Example of a splay
643   channel deposit overlying sandstone sheets within a mud-dominated succession from Location 11.

644   8) Schematic of the sandstone architectures present. Channel bodies generally decrease in thickness
645   from Geometry M through to I (see fig. 9). Geometry M, SA, IA and OS are considered to fall within the
646   sheet geometry classification, and I in the ribbon classification scheme of other authors. For geometric
647   dimension ranges of the channel bodies and storey surfaces see Table 1. Key characteristics are noted
648   next to each geometry defined. See text for discussion on how the different geometries have been
649   defined.

650   9) Graph showing the distribution of measured thicknesses for each geometry described (see text for
651   description of the different geometries). Box and whisker plots show the range, 1st and 3rd quartiles, and

652   the median for each geometry. Coloured stars denote the average thickness for each geometry. N=184
653   for whole dataset.

654   10) Example images of geometries M, SA and IA; A) Example image of a portion of geometry M from
655   Location 16. Note the lateral discontinuity of storey surface and extent of the channel body; B) Example
656   images of geometry SA with interpretation from Location 27. Note the floodplain intercalation that
657   separates the channel deposits which are laterally amalgamated; C) Image of an outcrop dominated by
658   geometry IA from Location 22; D) Close up example of geometry IA from Location 12 highlighting the
659   internal complexities and multistorey nature of the deposits.

660   11) Example images of geometries OS and I; A) Image from Location 25 showing the offset nature of
661   storey packages in geometry OS. Note the body is single storey in some places, yet multistorey in others;
662   B) Large scale view of a series of OS deposits from Location 25, note that they appear to have a broad
663   sheet like appearance; C) Example image of geometry I from Location 24.

664   12) A) Map showing the spatial distribution of the described geometries across the basin. Pie charts
665   depict the proportion of channels for each geometry from each sedimentary log taken. Ages taken from
666   Gingerich and Clyde (2001). B) Schematic demonstrating the transitional nature of the geometries from
667   geometry M through to I. Palaeocurrent direction is inferred to be from the top-left to bottom-right in
668   the schematic and does not relate to any specific area of the Bighorn Basin.

669   Figure 13) Examples of the described geometries in other sedimentary basins. A) Geometry M in the
670   Altos de Pica Formation, Chile B) Geometry SA in the Sariñena Formation, Spain C) Geometry IA in the
671   Morrison Formation, USA D) Geometry OS from the Sariñena Formation, Spain E) geometry I from the
672   Chinle Formation, Utah.

673   **TABLES**

674   Table 1 - Summary data for each geometry defined within this study. See text for facies association
675   descriptions. Brackets indicate the average for each category. Storey thickness are preserved thickness.

676   **References**

677   **Abdul, A.H., Hilgen, F.J., van Luijk, G.M., Sluijs, A., Kraus, M.J., Pares, J.M.,** and **Gingerich, P.D.,** (2008),
678   Astronomical climate control on paleosol stacking patterns in the upper Paleocene-lower Eocene
679   Willwood Formation, Bighorn Basin, Wyoming. *Geology,* **36**, 531–534.

680   **Abels, H.A., Kraus, M.J.,** and **Gingerich, P.D.,** (2013) Precession-scale cyclicity in the fluvial lower Eocene
681   Willwood Formation of the Bighorn Basin, Wyoming (USA). *Sedimentology*, **60**, 1467–1483.

682   **Allen, J.R.L.,** (1978) Studies in fluviatile sedimentation: an exploratory quantitative model for the
683   architecture of avulsion-controlled alluvial suites. *Sedimentary Geology*, **21**, 129–147.

684   **Allen, J.R.L.,** (1983) Studies in fluviatile sedimentation: Bars, bar-complexes and sandstone sheets (low-
685   sinuoisty braided streams) in the Brownstones (L.Devonian) Welsh Borders. *Sedimentary Geology*,
686   **33**, 237–293.

687   **Banham, S.G.,** and **Mountney, N.P.,** (2013) Controls on fluvial sedimentary architecture and sediment-
688   fill state in salt-walled mini-basins: Triassic Moenkopi Formation, Salt Anticline Region, SE Utah,
689   USA. *Basin Research*, **25**, 1–29.

690   **Blakey, R.C.,** and **Gubitosa, R.,** (1984) Controls of sandstone body geometry and architecture in the
691   Chinle Formation (Upper Triassic), Colorado Plateau. *Sedimentary Geology*, **38**, 51–86.

692   **Bown, T.M.,** and **Kraus, M.J.,** (1987) Integration of channel and floodplain suites, developmental
693   sequence and lateral relations of alluvial paleosols. *Journal of Sedimentary Petrology*, **57**, 587–601.

694   **Bown, T.M.,** and **Kraus, M.J.,** (1981) Lower Eocene alluvial paleosols (Willwood Formation, northwest
695   Wyoming, U.S.A) and their significance for paleoecology, paleoclimatology, and basin analyses.
696   *Palaeogeography, Palaeoclimatology, Palaeoecology*, **34**, 1–30.

697   **Bridge, J.S.,** (1993), Description and interpretation of fluvial deposits: a critical perspective.
698   *Sedimentology*, **40**, 801–810.

699   **Bridge, J.S.,** (2008) Numerical modelling of alluvial deposits: recent developments. In: *Analogue and*
700   *numerical modelling of sedimentary systems: from understanding to prediction. Special Publication*
701   *Number 40 of the IAS*, (Eds De Boer, P., Postma, G., van der Zwan, K., Burgess, P., and Kukla, P.)
702   97–138.

703   **Bridge, J.S.,** and **Leeder, M.R.,** (1979) A simulation model of alluvial stratigraphy. *Sedimentology*, **26**,
704   617–644.

705   **Bridge, J.S.,** and **Tye, R.S.,** (2000) Interpreting the dimensions of ancient fluvial channel bars, channels,
706   and channel belts from wireline-logs and cores. *AAPG Bulletin* , **84**, 1205–1228.

707   **Bristow, C.S.,** and **Best, J.L.,** (1993) Braided rivers: perspectives and problems. *Geological Society,*
708   *London, Special Publications*, **75**, 1–11.

709   **Cain, S.A.,** and **Mountney, N.P.,** (2009) Spatial and temporal evolution of a terminal fluvial fan system:
710   the Permian Organ Rock Formation, South-east Utah, USA. *Sedimentology*, **56**, 1774–1800.

711   **Cecil, B.C.,** (2003) The concept of autocyclic and allocyclic controls on sedimentation and stratigraphy,
712   emphasizing the climatic variables. In: *Climate controls on stratigraphy. SEPM Special Pbulication*
713   *Numer 77.* (Eds Cecil, B. C. and Edgar, T.N.) 13-20.

714   **Cecil, B.C.,** (2013) An overview and interpretation of autocyclic and allocyclic processes and the
715   accumulation of strata during the Pennsylvanian–Permian transition in the central Appalachian
716   Basin, USA. *International Journal of Coal Geology*, **119**, 21–31.

717   **Collinson, J.D.,** (1996) Alluvial sediments. In: *Sedimentary environments and facies* (Ed Reading, H.G.)
718   37-82.

719   **Corbeanu, R.M., Soegaard, K., Szerbiak, R.B., Thurmond, J.B., Mcmechan, G.A., Wang, D., Snelgrove,**
720   **S., Forster, C.B., Menitove, A.,** and **Corbeanu, R.M.,** (2001) Detailed internal architecture of a
721   fluvial channel sandstone determined from outcrop, cores, and 3-D ground-penetrating radar:
722   Example from the middle Cretaceous Ferron Sandstone, east-central Utah. *AAPG Bulletin*, **9**, 1583–
723   1608.

724   **Davies-Vollum, K.S.,** and **Kraus, M.J.,** (2001) A relationship between alluvial backswamps and avulsion
725   cycles: an example from the Willwood Formation of the Bighorn Basin, Wyoming. *Sedimentary*
726   *Geology*, **140**, 235–249.

727   **Davies-vollum, K.S.,** and **Wing, S.L.,** (1998) Taphononic, and climatic aspects of Eocene swamp deposits
728   (Willwood Formation, Bighorn Basin , Wyoming). *PALAIOS*, **13**, 28–40.

729 **Decelles, P.G.,** (2004) Late Jurassic to Eocene evolution of the Cordilleran thrust belt and foreland basin
730   system, western U.S.A. *American JournaL of Science*, **304**, 105–168.

731 **DeCelles, P.G., Gray, M.B., Ridgway, K.D., Cole, R.B., Pivnik, D.A., Pequera, N.,** and **Srivastava, P.,**
732   (1991) Controls on synorogenic alluvial-fan architecture, Beartooth Conglomerate (Palaeocene),
733   Wyoming and Montana. *Sedimentology*, **38**, 567–590.

734 **Dickinson, W.R., Klute, M.A., Hayes, M.J., Janecke, S.U., Erik, R., Mckittrick, M.A., Olivares, M.D.,**
735   **Klute, M.A.,** and **Hayes, M.J.,** (1988) Paleogeographic and paleotectonic setting of Laramide
736   sedimentary basins in the central Rocky Mountain region. *Geological Society of America Bulletin*,
737   100.

738 **Fisher, J. A., Nichols, G.J.,** and **Waltham, D. A**., (2007) Unconfined flow deposits in distal sectors of
739   fluvial distributary systems: Examples from the Miocene Luna and Huesca Systems, northern Spain.
740   *Sedimentary Geology*, **195**, 55–73.

741 **Foreman, B.Z.,** (2014) Climate-driven generation of a fluvial sheet sand body at the Paleocene-Eocene
742   boundary in north-west Wyoming (USA). *Basin Research*, **26**, 225–241.

743 **Friend, P.F.,** (1983) Towards the field classification of alluvial architecture or sequence. In: *Modern and*
744   *ancient fluvial systems: International Association of Sedimentologists, Special Publication 6* (Eds
745   Collinson, J.D. and Lewin, J), 345–354.

746 **Friend, P.F., Slater, M.J.,** and **Williams, R.C.,** (1979) Vertical and lateral building of river sandstone
747   bodies, Ebro Basin, Spain. *Journal of the Geological Society*, **136**, 39–46.

748 **Gibling, M.R.,** (2006) Width and thickness of fluvial channel Bodies and valley fills in the geological
749   record: A literature compilation and classification. *Journal of Sedimentary Research*, **76**, 731–770.

750 **Gingerich, P.D.,** (1983) Paleocene-Eocene faunal zones and a preliminary analysis of Laramide structural
751   deformation in the Clark's Fork Basin, Wyoming. In: *34th Annual Field conference, Wyoming*
752   *Geological Association Guidebook*, 185–195.

753 **Gingerich, P.D.,** (2003) Mammalian responses to climate change at the Paleocene-Eocene boundary:
754   Polecat Bench record in the northern Bighorn Basin, Wyoming. *Geological Society of America*
755   *Special Papers*, **369**, 463–478.

756 **Gingerich, P.D. and Clyde, W.C.,** (2001) Overview of mammalian biostratigraphy in the Paleocene-
757   Eocene Fort Union and Willwood Formations of the Bighorn and Clarks Fork Basins. *University of*
758   *Michigan papers on paleontology,* **33**, 1-14.

759 **Gulliford, A.R., Flint, S.S.,** and **Hodgson, D.M.,** (2014) Testing Applicability of Models Of Distributive
760   Fluvial Systems Or Trunk Rivers In Ephemeral Systems: Reconstructing 3-D Fluvial Architecture In
761   the Beaufort Group, South Africa. *Journal of Sedimentary Research*, **84**, 1147–1169.

762 **Hickey, L.J.,** and **Yuretich, R.,** (1997) The Belfry Member of the Fort Union Formation, an allocyclic
763   lacustrine deposit of middle Paleocene agin in the Bighorn Basin, Montana and Wyoming. In:
764   *Bighorn Basin: 50 years on the Frontier: Evolution of the geology of the Bighorn Basin*: *Fieldtrip*
765   *Symposium*, 38–42.

766 **Hirst, J.P.P.,** (1991) Variations in alluvial architecture across the Oligo-Miocene Huesca fluvial system,
767   Ebro Basin, Spain. In: *The three dimensional facies architecture of terrigenous clastic sediments and*
768   *its implications for hydrocarbon discovery and recovery. Concepts in Sedimentology and*

769 *Paleontology* (Eds: Miall, A.D. and Tyler, N.), 111–121.

770 **Hornung, J.,** and **Aigner, T.,** (1999) Reservoir and aquifer characterization of fluvial architectural
771 elements: Stubensandstein, Upper Triassic, southwest Germany. *Sedimentary Geology*, 129, 215–
772 280.

773 **Huerta, P., Armenteros, I.,** and **Silva, P.G.,** (2011) Large-scale architecture in non-marine basins: the
774 response to the interplay between accommodation space and sediment supply, *Sedimentology*, **58**,
775 1716–1736.

776 **Jackson, R.G.,** (1975) Hierarchical attributes and a unifying model of bed forms composed of
777 cohesionless material and produced by shearing flow. *Bulletin of the Geological Society of America*,
778 **86**, 1523–1533.

779 **Jones, H.L.,** and **Hajek, E.A.**, (2007) Characterizing avulsion stratigraphy in ancient alluvial deposits.
780 *Sedimentary Geology*, 202, 124–137.

781 **Kennett, J.P.,** and **Stott, L.D.,** (1991) Abrupt deep-sea warming, paleoceanographic changes and benthic
782 extinctions at the end of the Palaeocene. *Nature,* **353**, 225–228.

783 **Kraus, M.J.,** (1980) Genesis of a fluvial sheet sandstone, Willwood Formation, northwest Wyoming.
784 *University of Michigan Papers on Paleontology*, **24**, 87–94.

785 **Kraus, M.J.,** (1985) Early Tertiary quartzite conglomerates of the Bighorn Basin and their significance for
786 paleogeographic reconstruction of northwest Wyoming. In: *Cenozoic Paleogeography of West-*
787 *central United States, Rocky Mountain Section of the SEPM* (Eds: Flores, R.M. and Kaplan, S.S.), 71–
788 91.

789 **Kraus, M.J.,** (1987) Integration of channel and floodplain suites, II Vertical relations of alluvial paleosols.
790 *Journal of Sedimentary Petrology*, **57**, 602–612.

791 **Kraus, M.J.,** (1996) Avulsion deposits in Lower Eocene alluvial rocks, Bighorn Basin, Wyoming. *Journal of*
792 *Sedimentary Research,* **66**, 354–363.

793 **Kraus, M.J.,** (1999) Paleosols in clastic sedimentary rocks: their geologic applications. *Earth-Science*
794 *Reviews*, **47**, 41–70.

795 **Kraus, M.J.,** (2001) Sedimentology and depositional setting of the Willwood Formation in the Bighorn
796 and Clarks Fork Basins In: *Paleocene-Eocene Stratigraphy and Biotic change in the Bighorn and*
797 *Clarks Fork Basins, Wyoming, University of Michigan Papers Paleontology, No 33* (Ed: Gingerich,
798 P.D.), 15–28.

799 **Kraus, M.J.,** and **Bown, T.M.,** (1993) Palaeosols and sandbody prediction in alluvial sequences.
800 *Geological Society, London, Special Publications*, **73**, 23–31.

801 **Kraus, M.J.,** and **Gwinn, B.,** (1997) Facies and facies architecture of Paleogene floodplain deposits,
802 Willwood Formation, Bighorn Basin, Wyoming, USA. *Sedimentary Geology*, **114**, 33–54.

803 **Kraus, M.J.,** and **Wells, T.M.,** (1999) Recognizing avulsion deposits in the ancient stratigraphical record.
804 In: *Fluvial Sedimentology 6. Special publication of the International Association of Sedimentologists*
805 (Eds: Smith, N.D. and Rogers, J.), 251–268.

806 **Kraus, M.J.,** and **Davies-Vollum, K.S.,** (2004) Mudrock-dominated fills formed in avulsion splay channels:
807 Examples from the Willwood Formation, Wyoming. *Sedimentology*, 51, 1127–1144.

808 **Kraus, M.J.,** and **Hasiotis, S.T.,** (2006) Significance of Different Modes of Rhizolith Preservation to
809   Interpreting Paleoenvironmental and Paleohydrologic Settings: Examples from Paleogene
810   Paleosols, Bighorn Basin, Wyoming, U.S.A. J*ournal of Sedimentary Research*, **76**, 633–646.

811 **Kraus, M.J.,** and **Riggins, S.,** (2007) Transient drying during the Paleocene–Eocene Thermal Maximum
812   (PETM): Analysis of paleosols in the bighorn basin, Wyoming: *Palaeogeography, Palaeoclimatology,*
813   *Palaeoecology*, **245**, 444–461.

814 **Kraus, M.J., McInerney, F.A., Wing, S.L., Secord, R., Baczynski, A.A.,** and **Bloch, J.I.**, (2013)
815   Paleohydrologic response to continental warming during the Paleocene–Eocene Thermal
816   Maximum, Bighorn Basin, Wyoming. *Palaeogeography, Palaeoclimatology, Palaeoecology*, **370**,
817   196–208.

818 **Kraus, M.J., Woody, D.T., Smith, J.J.,** and **Dukic, V.,** (2015) Alluvial response to the Paleocene–Eocene
819   Thermal Maximum climatic event, Polecat Bench, Wyoming (U.S.A.). *Palaeogeography,*
820   *Palaeoclimatology, Palaeoecology*, **435**, 177–192.

821 **Leeder, M.R.,** (1978) A quantitative stratigraphoc model for alluviam with special reference to channel
822   deposit density and interconnectedness. *Canadian Society of Petroleum Geologist Memoir 5*, 587–
823   596.

824 **Leleu, S., Hartley, A.J.,** and **Williams, B.P.J.,** (2009) Large-Scale Alluvial Architecture and Correlation in a
825   Triassic Pebbly Braided River System, Lower Wolfville Formation (Fundy Basin, Nova Scotia,
826   Canada). *Journal of Sedimentary Research*, **79**, 265–286.

827 **Lillegraven, J.A.**, (2009) Where was the western margin of northwestern Wyoming's Bighorn Basin late
828   in the early Eocene? *Papers on Geology, Vertebrate Paleontology, and Biostratigraphy in Honor of*
829   *Michael O. Woodburne*, **65**, 37–81.

830 **Miall, A.D.,** (1985) Architectural-element analysis: A new method of facies analysis applied to fluvial
831   deposits. *Earth-Science Review*s, **22**, 261–308.

832 **Miall, A.D.,** (1988) Architectural elements and bounding surfaces in fluvial deposits: Anatomy of the
833   Kayenta Formation (Lower Jurassic), Southwest Colorado. *Sedimentary Geology*, **55**, 233-262.

834 **Miall, A.D.,** (1994) Reconstructing fluvial macroform architecture from two-dimensional outcrops:
835   examples from the Castlegate Sandstone, Book Cliffs, Utah. *Journal of Sedimentary Research*, **64**,
836   146–158.

837 **Miall, A.D.,** (1996) T*he Geology of Fluvial deposts: Sedimentary facies, basin analysis, and petroleum*
838   *geology*. Springer-verlag, New York, 582.

839 **Miall, A.D.,** (2016) The valuatin of unconformities. *Earth-science Reviews*, **163**, 22-71.

840 **Neasham, J.W.,** and **Vondra, C.F.,** (1972) Stratigraphy and petrology of the Lower Eocene Willwood
841   Formation, Bighorn Basin, Wyoming. *Geological Society of America Bulletin*, **83**, 2167–2180.

842 **Nichols, G.J.,** and **Fisher, J.A.,** (2007) Processes, facies and architecture of fluvial distributary system
843   deposits. *Sedimentary Geology*, **195**, 75–90.

844 **Owen, A., Nichols, G.J., Hartley, A.J., Weissmann, G.S.,** and **Scuderi, L.A.,** (2015a) Quantification of a
845   distributive fluvial system: The Salt Wash DFS of the Morrison Formation, SW USA. *Journal of*
846   *Sedimentary Research*, **85**, 544-561.

847 **Owen, A., Nichols, G.J., Hartley, A.J., and Weissmann, G.S.,** (2015b) Vertical trends within the
848   prograding Salt Wash distributive fluvial systems, SW United States. *Basin Research,* 1-17.

849 **Potter, P.,** (1967) Sand Bodies and Sedimentary Environments: A Review. *AAPG Bulletin*, **3**, 337–365.

850 **Pranter, M.J.,** and S**ommer, N.K.,** (2011) Static connectivity of fluvial sandstones in a lower coastal-plain
851   setting: An example from the Upper Cretaceous lower Williams Fork Formation, Piceance Basin,
852   Colorado. *AAPG Bulletin*, **95**, 899–923.

853 **Ramos, A.,** and S**opena, A.,** (1983) Gravel bars in low-sinuosity streams (Permian and Triassic, central
854   Spain). In: *Modern and Ancient Fluvial Systems: International Association of Sedimentologists,*
855   *Special Publication 6* (Eds: Collinson, J.D. and Lewin, J), 301–312.

856 **Retallack, G.J.,** (2001) *Soils of the past. An introduction to paleopedology*: Blackwell Science, 520.

857 **Rouse, J.T.,** (1937) Genesis and structural relationships of the Absaroka volcanic rocks, Wyoming.
858   *Bulletin of the Geological Society of America*, **48**, 1257–1296.

859 **Rust, B.R.,** (1972) Structure and process in a braided river. *Sedimentology*, **18**, 221-245.

860 **Seeland, D.,** (1998) Late Cretaceou , Paleocene, and Early Eocene Paleogeography of the Bighorn Basin
861   and Northwestern Wyoming. In: Cretaceous and Lower tertiary Rocks of the Bighorn Basin,
862   Wyoming and Montana; 49th Annual Field Conference Guidebook, 1–29.

863 **Shen, Z., Törnqvist, T.E., Mauz, B., Chamberlain, E.L., Nijhuis, A.G.,** and **Sandoval, L.,** (2015) Episodic
864   overbank deposition as a dominant mechanism of floodplain and delta-plain aggradation. *Geology*,
865   **43**, 10, 875–878.

866 **Singh, H., Parkash, B.,** and **Gohain, K.,** (1993) Facies analysis of the Kosi megafan deposits. S*edimentary*
867   *Geology*, **85**, 87–113.

868 **Snyder, W.S., Dickinson, W.R.,** and **Silberman, M.L.,** (1976) Tectonic implications of space-time patterns
869   of Cenozoic magmatism in the Western United States. *Earth and Planetary Science Letters*, **32**, 91–
870   106.

871 **Sundell, K.A.,** (1990) Sedimentation and tectonics of the Absaroka Basin of northwestern wyoming. In:
872   *Wyoming sedimentation and Tectonics, 41st Annial Field Conference Guidebook*, 105–122.

873 **Weissmann, G.S., Hartley, A.J., Nichols, G.J., Scuderi, L.A., Olson, M.E., Buehler, H.,** and **Banteah, R.,**
874   (2010) Fluvial form in modern continental sedimentary basins: Distributive fluvial systems.
875   *Geology*, **38**, 39–42.

876 **Weissmann, G.S., Hartley, A.J., Scuderi, L.A., Nichols, G.J., Davidson, S.K., Owen, A., Atchley, S.C.,**
877   **Bhattacharyya, P., Ghosh, P., Nordt, L.C., Michel, L.,** and **Tabor, N.J.,** (2013) Prograding
878   distributive fluvial systems - geomorphic models and ancient examples. In: *New Frontiers in*
879   *Paleopedology and Terrestrial paleoclimatology. SEPM Special Number 104* (Eds: Dreise, S.G.,
880   Nordt, L.C., and McCarthy, P.L.), 131–147.

881 **Weissmann, G.S., Hartley, A.J., Scuderi, L.A., Nichols, G.J., Owen, A., Wright, S., Felicia, A.L., Holland,**
882   **F.,** and **Anaya, F.M.L.,** (2015) Fluvial geomorphic elements in modern sedimentary basins and their
883   potential preservation in the rock record: A review. *Geomorphology*, **250**, 187–219.

884 **Willis, B.J.,** and **Behrensmeyer, A. K.,** (1995) Fluvial systems in the Siwalik Miocene and Wyoming
885   Paleogene. *Palaeogeography, Palaeoclimatology, Palaeoecology*, **115**, 13–35.

886 **Wilson, A., Flint, S., Payenberg, T., Tohver, E.,** and **Lanci, L.,** (2014) Architectural Styles and
887   Sedimentology of the Fluvial Lower Beaufort Group, Karoo Basin, South Africa. *Journal of*
888   *Sedimentary Research*, **84**, 326–348.

889 **Wing, S.L.,** and **Currano, E.D.,** (2013) Plant response to a global greenhouse event 56 million years ago.
890   *American Journal of Botany*, **100**, 1234–54.

891 **Wing, S.L., Harrington, G.J., Smith, F.A., Bloch, J.I., Boyer, D.M.,** and **Freeman, K.H.,** (2005) Transient
892   floral change and rapid global warming at the Paleocene-Eocene boundary. *Science*, **310**, 993–996.

893 **Yuretich, R.F., Hickey, L.J., Gregson, B.P.,** and **Hsia, Y.L.,** (1984) Lacustrine deposits in the Paleocene
894   Fort Union Formation, northern Bighorn Basin, Montana. *Journal of Sedimentary Petrology*, **54**,
895   836–852.

896

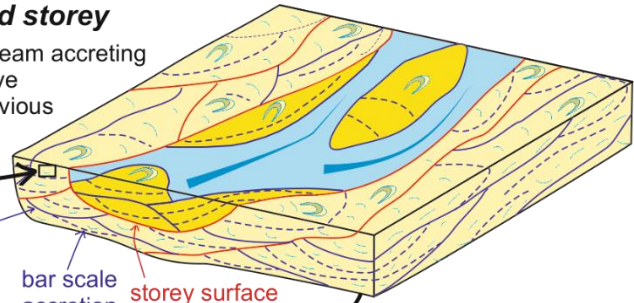| Geometry	Facies associations present	Maximum measured lateral extent (Km)	Thickness of channel fill body (m)	Storey thickness (m)	Number of storeys (m)
M	1, 2	5.5	5.7– 47.5 (21.4)	1.4-47.5 (10.1)	Up to 5 (2.1)
SA	1, 2, 3	3.5	1- 44.5 (7.5)	1-30.3 (5.7)	Up to 3 (1.3)
IA	2, 3, 4	3	4.1 – 27.6 (11.0)	1.5-14.3 (4.6)	Up to 4 (2.4)
OS	3, 4	1	2.4- 13.7 (7.7)	0.3-7.1 (3.8)	Up to 3 (2)
I	3, 4	1	1.7- 11.4 (4.2)	N/A	N/A

897

Bedforms - ripples/dunes
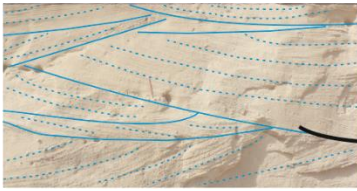
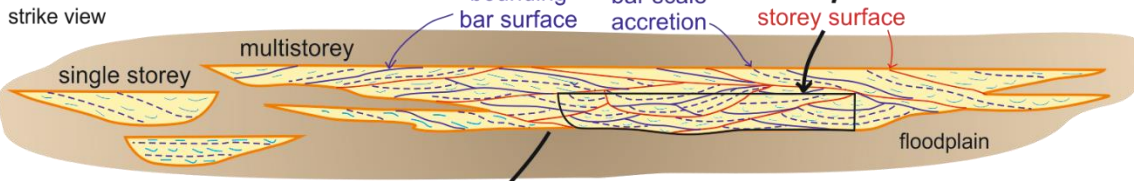bedform sets and co-sets

Barform and storey
- lateral/downstream accreting
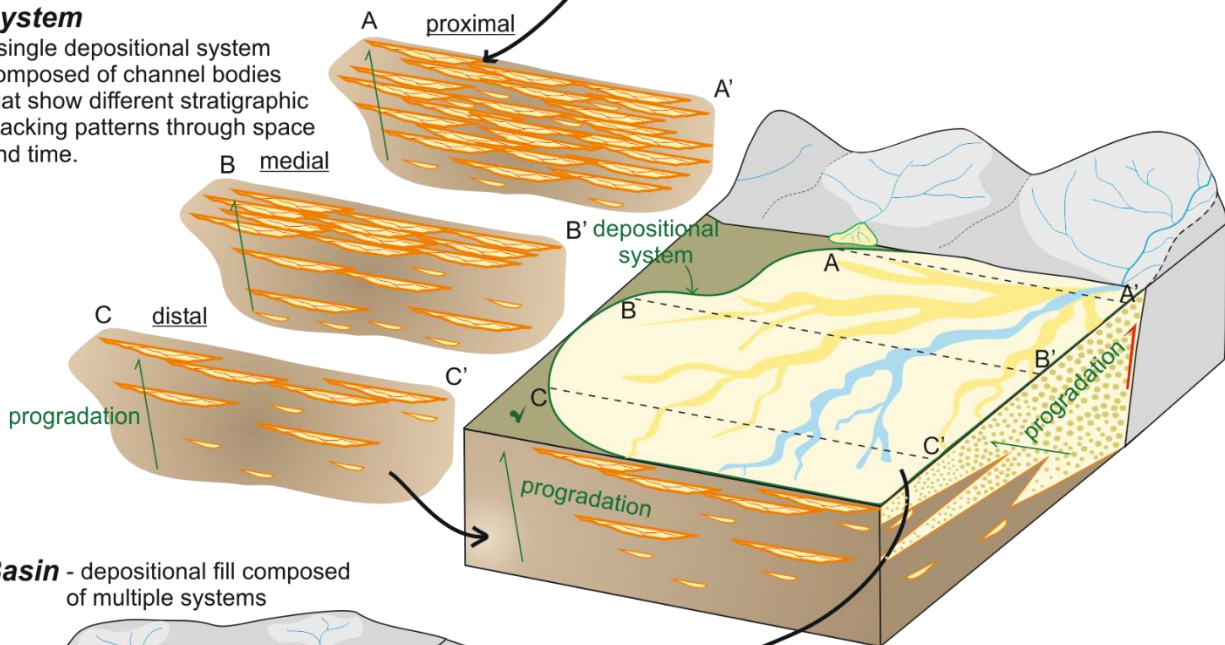- incision of active channel into previous deposits

bounding bar surface
bar scale accretion
storey surface

Channel body - single/multiple channel fills encased within floodplain material

strike view

bounding bar surface
bar scale accretion
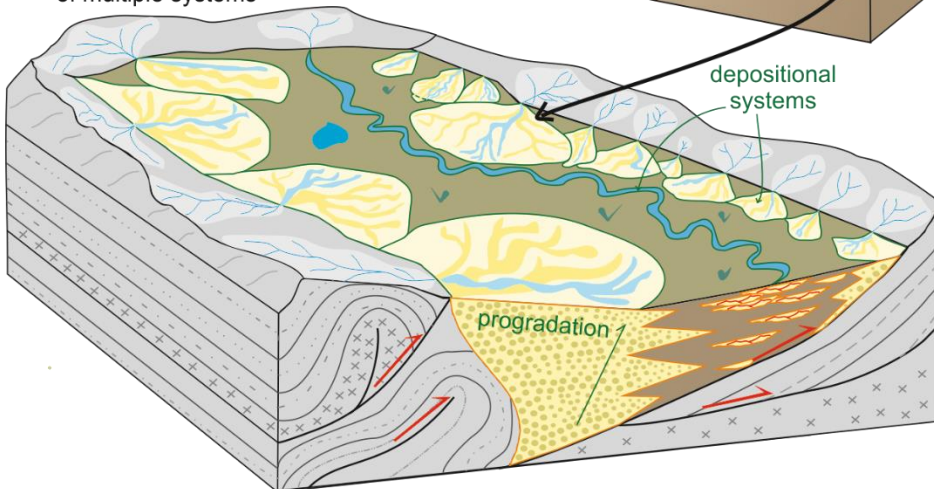storey surface

multistorey
single storey
floodplain

System
- single depositional system composed of channel bodies that show different stratigraphic stacking patterns through space and time.

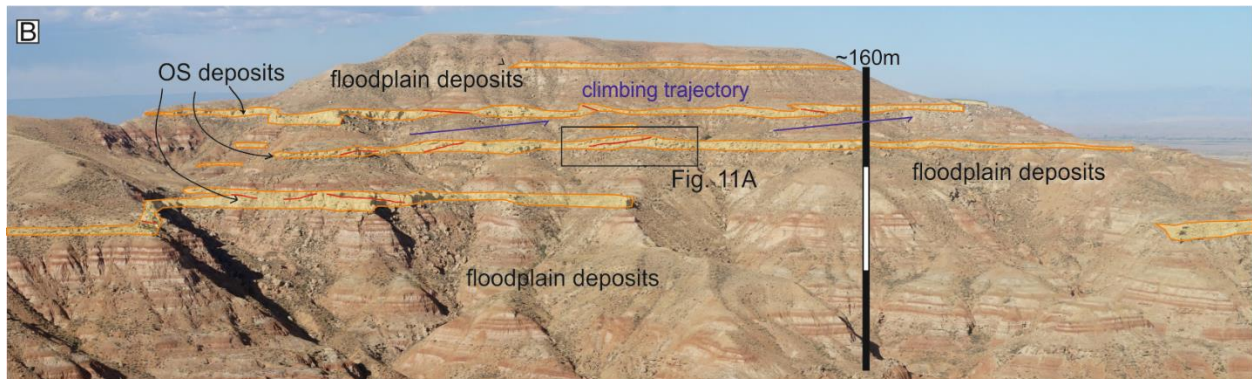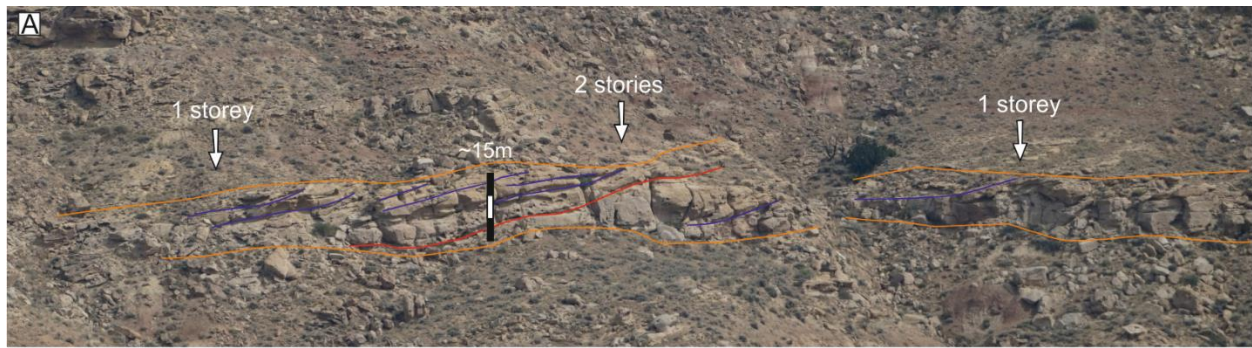A   proximal   A'
B   medial   B' depositional system
C   distal   C'

progradation
progradation
progradation

depositional system
A   A'
B   B'
C   C'
progradation

Basin - depositional fill composed of multiple systems

depositional systems

progradation

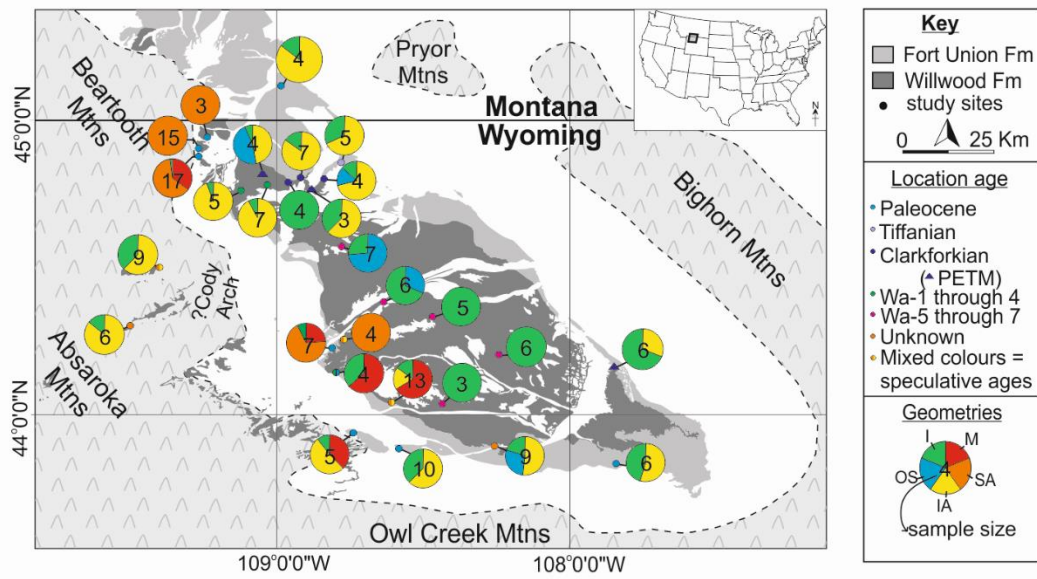**Key surfaces**
bedforms
barforms
storey
channel body
system

898

A

1 storey

2 stories

~15m

1 storey

B

OS deposits

floodplain deposits

climbing trajectory

~160m

Fig. 11A

floodplain deposits

floodplain deposits

C

~3.5m

multiple bars

Geometry I

Key surfaces

| bedforms | storey |
| barforms | channel body |

899